Int. J. Heat Mass Transfer. Vol. 18, pp. 615–622. Pergamon Press 1975. Printed in Great Britain

NEW THEORIES OF THE A-AXIS GROWTH OF ICE CRYSTALS

H. C. SIMPSON, G. C. BEGGS and J. DEANS
Department of Thermodynamics and Fluid Mechanics, University of Strathclyde, 75 Montrose Street, Glasgow, Scotland

(*Received* 27 *April* 1974 *and in revised form* 27 *September* 1974)

Abstract—New theories are presented for the *A*-axis growth rate of ice crystals in flowing water or saline solutions with a high degree of subcooling. An existing theory, based on laminar boundary-layer flow over the front stagnation point of the growing crystal is believed to be unsatisfactory because the assumptions of first-order boundary-layer theory are inadmissible at the low crystal tip Reynolds number ($\approx 3 \times 10^{-3}$) encountered.

Two models have been developed, one based on an analysis for creeping flow over the crystal tip, the other on conduction of heat along the growing crystal, this heat then being removed by forced convection from the relatively large flat faces of the crystal. These models give much closer agreement with the experimental results for *A*-axis growth in pure water.

When modified to allow for salt diffusion from the ice tip in creeping flow, both models also give improved estimates of growth rates in saline solutions although the improvement is not so pronounced as for growth in pure water.

NOMENCLATURE

v, *A*-axis crystal growth rate [cm/s];
V, main stream centre line velocity [cm/s];
T_m, melting point of water [K];
T_∞, bulk temperature of liquid [K];
T_i, temperature at crystal interface [K];
ΔT, sub-cooling below water freezing point [K];
ΔT_s, sub-cooling below main stream freezing point [K];
W_∞, mass fraction of salt in main stream;
W_i, mass fraction of salt at the crystal interface;
λW_∞, freezing point depression at concentration W_∞ [K];
ρ_s, density of brine [kg/m^3];
ρ_i, density of ice [kg/m^3];
κ, thermal diffusivity of brine [m^2/s];
D, mass diffusivity of brine [m^2/s];
ν, kinematic viscosity of brine [m^2/s];
R, radius of curvature of crystal tip [m];
R_0, crystal tip radius for maximum growth [m];
L, latent heat of ice [J/kg];
C_p, specific heat of ice [J/kg K];
γ, interfacial energy [mJ/m^2];
Pr, Prandtl number of brine;
Re, $\left(=\frac{VR}{\nu}\right)$, Reynolds number at crystal tip;
Sc, Schmidt number of brine;
$\pi'(Pr)$, dimensionless temperature gradient at crystal surface with no mass transfer;
$\pi'(Sc)$, dimensionless concentration gradient at crystal surface with no mass transfer;
$\delta_v, \delta_T, \delta_m$, momentum, thermal and diffusion film thickness for laminar boundary-layer model [m];
k_i, k_l, thermal conductivity of ice and brine [W/m^2 K].

1. INTRODUCTION

IN THE desalination of sea or brackish water by freezing, the size distribution and shape of the ice crystals growing in the turbulent brine solution are determined by their local environment and surface kinetics. A thorough understanding of the mechanism of growth in brine is essential for improving the freezing process.

The literature on ice crystal nucleation and growth has been reviewed by Deans [1]. Ice crystals form as thin platelets with a fast growing *A*-axis in the plane of the platelet and a slow growing *C*-axis at right angles to it. For the low temperature differences between ice and brine used in practice, *A*-axis growth rates have been measured with the ice crystal growing in a flowing stream of brine by Bukina [2], Farrar and Hamilton [3] and Fernandez [4]. The results obtained indicate that the *A*-axis growth rate is heat transfer controlled. Fernandez [4], working under Barduhn, applied laminar boundary-layer theory, for flow round the front stagnation point of the crystal, to predict the *A*-axis growth rate but used the interfacial tension γ between ice and brine as an effective fitting factor to force agreement between theory and experiment. In later papers, Barduhn's group elaborated the theory to allow for diffusion of salt away from the growing crystal [5] but this theory was inadequate to explain quantitatively the effect of salt. In addition, it appeared that the assumptions inherent in the boundary-layer theory were not reasonable when applied to a flow of such low Reynolds number.

An experimental and theoretical study was thus carried out by Deans [1]. An outline of the experimental method and results for both *A*-axis and *C*-axis growth has been given by Simpson *et al.* [6]. The main purpose of this paper is to present a theory for *A*-axis growth which is believed to be superior to that based

on stagnation flow boundary-layer theory and for this reason attention is concentrated on measurements of the A-axis growth in brine and water for temperature differences in the range 0·1–1·0 K.

2. EXPERIMENTAL APPROACH

A drawing of the experimental equipment is shown in Fig. 1 and full details have been provided by Deans [1] and by Simpson *et al.* [6]. The rig consisted

The growing crystal was observed and photographed through twin periscopes made from evacuated glass tubing sealed with optical glass. The A-axis growth rates were obtained from the position of the crystal tip at various times, the position being recorded by a low power microscope and a reflex camera positioned at the top of the viewing periscope and readings being taken in brine concentration 0–6 per cent for sub-coolings between 0·1 and 1·0 K at flow velocities of

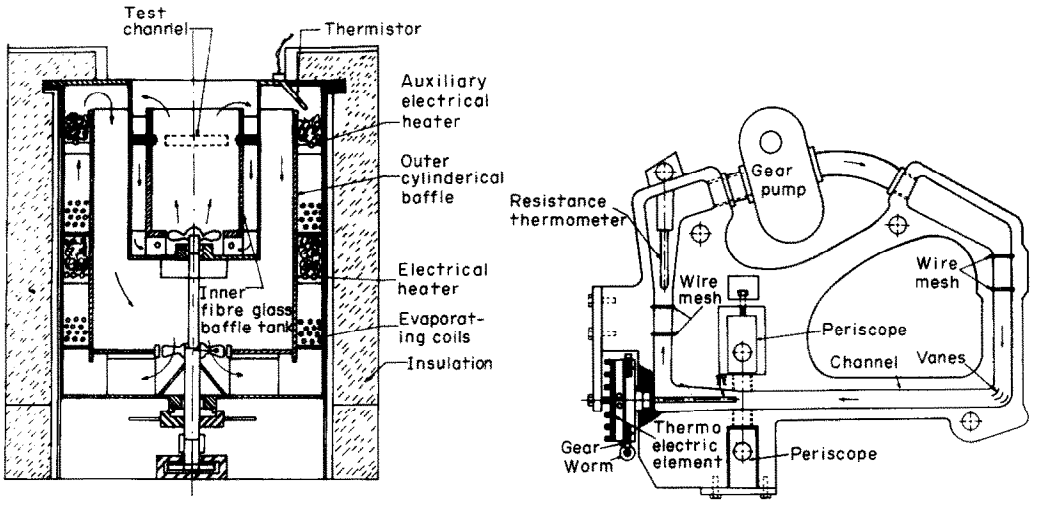

FIG. 1. Temperature control bath and test channel.

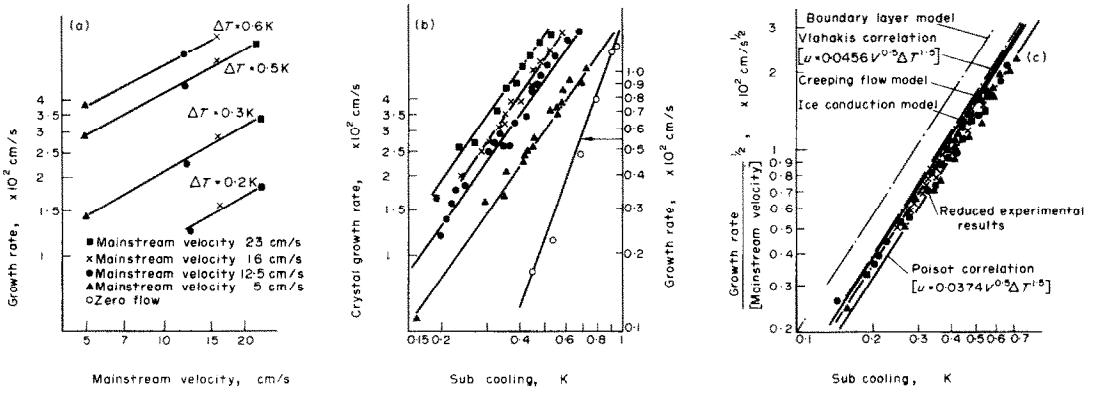

FIG. 2. Ice crystal growth rates in water.

essentially of a small flow channel, 15 mm square in section, machined from a solid block of perspex, with the top and bottom walls of the channel formed from sheet copper bonded to the perspex. Water or brine was circulated round the channel by a variable speed gear pump at four velocities in the range 5 cm/s to 23 cm/s. The brine in the flow circuit was maintained within ±0·001 K at a temperature between 0 and −6°C by immersing it in a constant temperature control bath. The ice crystal was nucleated by a thermo-electric cooling unit, from the end of a 60 mm long thin walled glass capillary tube filled with water or brine and arranged so that crystal growth occurred into the flowing stream.

5 and 12·5 cm/s for both water and brine and at flow velocities of 16 and 23 cm/s for water only.

3. EXPERIMENTAL RESULTS

The A-axis growth rate v, for ice in pure water at the condition specified above, is shown in Fig. 2. Figure 2(b) shows that $v \propto (\Delta T)^n$ where $n \simeq 1{\cdot}45$ at all four stream velocities, although, as this figure also shows, the growth velocity at zero flow velocity indicates an index $n = 3$ and a growth rate an order of magnitude lower than for the flowing streams. Figure 2(a) shows that v varies with stream velocity V according to the relation $v \propto V^{1/2}$ and when $v/V^{1/2}$ is plotted against ΔT the data reduce to a single line which can be represented to

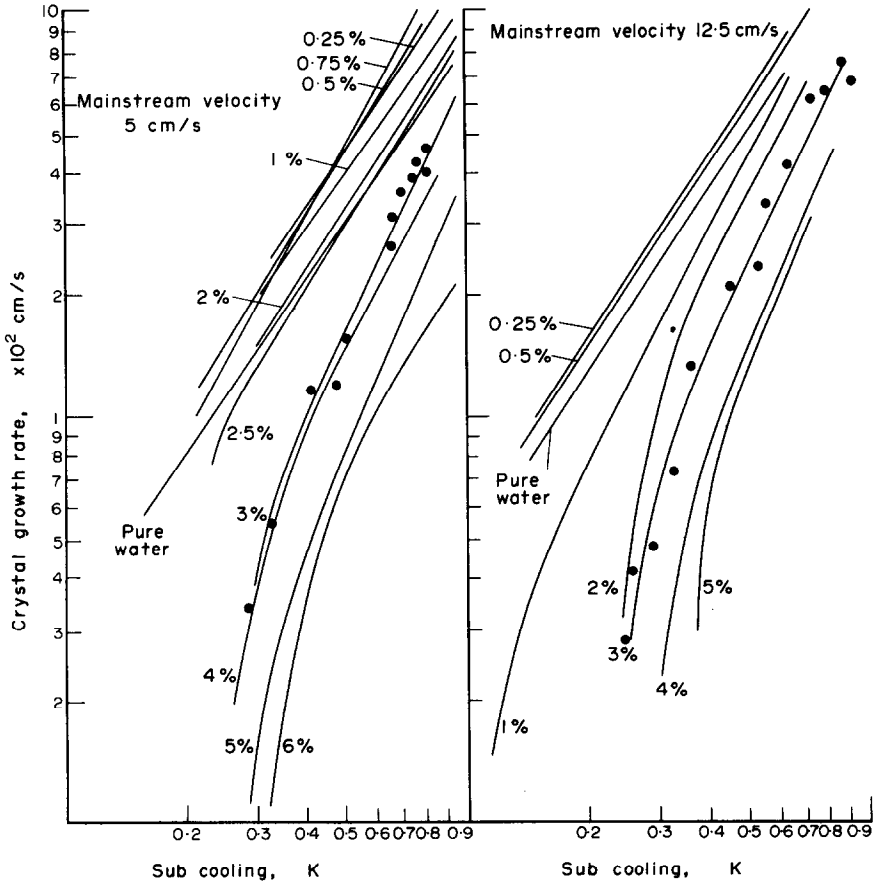

FIG. 3. Ice crystal growth rates in brine.

within ± 5 per cent by the equation

$$v = 0{\cdot}038V^{1/2}\Delta T^{3/2}. \qquad (1)$$

It can also be seen from Fig. 2(c) that the current data show good agreement with the empirical correlations of both Poisot [7] and Vlahakis [8].

The more complex data, for ice crystal growth in flowing brine, are shown in Fig. 3, in which crystal growth rate v is plotted against ΔT for brine velocities of 5 and 12·5 cm/s at mainstream concentration W_∞ between 0 and 6 per cent by weight. For clarity, individual test points are shown for one salt concentration only. At the higher range of ΔT a relationship $v \propto \Delta T^n$ is obtained for brine as well as for water but at salt concentrations greater than 1 per cent the growth rate decreases more rapidly with decrease of sub-cooling. However, our attention is directed to the data for higher values of ΔT and lower brine concentration where $v \propto \Delta T^n$.

With increasing salt concentration the growth rate passes through a maximum, as shown in Fig. 4 for a sub-cooling of 0·6 K, which occurs at concentrations of 0·3 per cent at 12·5 cm/s and 0·6 per cent at 5 cm/s the maximum growth velocities being about 25 and 50 per cent greater than the corresponding pure water growth velocities. With further increase of salt concentration the growth rate decreases, falling to about 25 per cent of the pure water value with a 6 per cent brine.

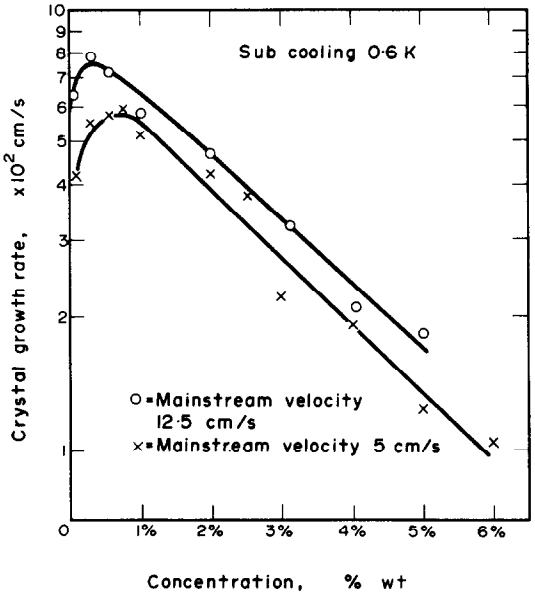

FIG. 4. Variation of ice crystal growth rate with concentration.

The existence of maxima in growth rates with salt concentration has been observed by other investigators, Tamman and Buchner [9], Lindenmeyer [11] and Farrar and Hamilton [3]. However, the phenomenon remains largely unexplained.

4. THEORY OF THE A-AXIS GROWTH

4.1 *Laminar boundary-layer flow*

The results in Figs. 2 and 3 for A-axis growth show that

$$v = A_1 V^{1/2} \Delta T^n \tag{2}$$

where n increases from 1·5 for pure water to 2·2 for the 5 per cent solution and where the constant A_1 decreases as the salt concentration increases. The dependence of the crystal growth rate v on $V^{1/2}$, where V is the stream velocity, suggests that the growth rate might be determined by the heat and mass transfer through the laminar boundary layer surrounding the front of the crystal. This was the approach followed by Barduhn *et al.* Using standard solutions for the laminar boundary-layer flow over the front stagnation point of a cylinder, Bird, Stewart and Lightfoot [10] and assuming the thicknesses of the thermal and mass diffusion boundary layers to be small compared with the momentum boundary layer, so that the velocity gradient can be taken to be linear in these diffusion layers, Fernandez [5] showed that the crystal growth rate was given by,

$$\left(\frac{v}{V}\right) = \left(\frac{\rho_s}{\rho_i}\right)\left(\frac{\kappa}{\nu}\right)\left(\frac{\nu}{VR}\right)^{1/2} \frac{\pi'(Pr)}{1 + \left(\frac{\kappa}{D}\right)\left|\frac{\pi'(Pr)}{\pi'(Sc)}\right|\left(\frac{C_p \lambda W_\infty}{L}\right)} \times \frac{C_p(\Delta T_s - \beta/R)}{L} \tag{3}$$

where W_∞ is the mass concentration of salt in the main stream and $\Delta T_s = T_m - T_\infty - \lambda W_\infty$ is the sub-cooling below the melting point of the main stream, due allowance being made in the β/R term for the curvature of the crystal. However, the radius of curvature R of the crystal was unknown although equation (3) implies

$$v \propto \frac{\Delta T_s - (\beta/R)}{R^{1/2}}.$$

In common with other investigators of crystal growth, Fernandez assumed that the crystal adjusted itself so that the crystal radius R became the value R_0 at which maximum growth rate occurred. Assuming then

$$\frac{\partial v}{\partial R} = 0.$$

$$R_0 = \frac{3\beta}{\Delta T_s} = \frac{3\gamma T_m}{\rho_i L \Delta T_s} \tag{4}$$

and

$$\left(\frac{v}{V}\right) = \frac{2}{3}\left(\frac{\rho_s}{\rho_i}\right)\left(\frac{\kappa}{\nu}\right) \frac{\pi'(Pr)}{1 + \left(\frac{\kappa}{D}\right)\left|\frac{\pi'(Pr)}{\pi'(Sc)}\right|\left(\frac{C_p \lambda W_\infty}{L}\right)} \times \left(\frac{\rho_i L \nu \Delta T_s}{3\gamma T_m V}\right)^{1/2} \frac{C_p \Delta T_s}{L}. \tag{5}$$

Equation (5) implies equation (2) with A_1 decreasing as the salt concentration increases, and qualitative agreement exists between theory and experiment.

However, examination of equation (5) shows that the boundary-layer theory is unsatisfactory on two counts. First, Fernandez used the interfacial tension γ as a fitting factor. The best value for the growth data was 53 mJ/m^2, $2\frac{1}{2}$ times the presently accepted value of 20 $\pm$2 mJ/m^2 given by Lindenmeyer [11]. Second, if a typical value of ΔT of 0·3 K is substituted in equation (4), the radius of curvature R_0 of the tip is found to be 20×10^{-6} cm, implying a tip Reynolds number of about 3×10^{-3}. Although the theoretical value of the crystal tip radius is small, the value agrees with that calculated by Fernandez [4]. Also, although experimental determination of the tip radius is extremely difficult, photographs taken by Nakamura [16] suggest the experimental and theoretical values have the same order of magnitude. The ratio of the momentum boundary-layer thickness δ_v to the radius of curvature R_0 is approximately $2/Re^{1/2}$ giving a ratio $\delta v/R_0$ of about 36·5. This shows that the boundary-layer thickness δ_v is much greater than the tip radius of curvature, suggesting that the assumptions of the first-order boundary-layer theory used above are not permissible. Comparable calculations, Deans [1], give a thermal film thickness ratio δ_T/R_0 of about 11 and a diffusion film thickness δ_m/R_0 of about 2·3.

This suggested that the boundary-layer approach should be abandoned and that creeping flow should be considered because of the low tip Reynolds numbers involved in the crystal growth.

4.2 *Creeping flow*

Creeping flow round bluff bodies presents problems of great mathematical complexity, Batchelor [12]. The overall shape of the body has a strong influence on the local flow pattern at the front stagnation point even for a given radius of curvature. For this reason, the dimensionless stream function $\psi' = \psi/\nu$ for creeping flow about a parabolic cylinder expressed as a function of parabolic co-ordinates ξ and η was used in conjunction with the numerical solutions of the Navier–Stokes equation by Davis [13] and Dennis and Walsh [14]. This implies,

$$\psi' = A_2 \xi(\eta - Re^{1/2}) \quad \text{with} \quad A_2 = 0{\cdot}267 \tag{6}$$

and the parabolic co-ordinates are related to the Cartesian co-ordinates, centred on the focus of the crystal parabola as shown in Fig. (5), by the expressions

$$x = \frac{\nu}{2V}(\xi^2 - \eta^2), \quad y = \frac{\nu}{V}\xi\eta.$$

The two-dimensional equation of heat transfer for the fluid near the surface of the crystal is given in Cartesian coordinates by,

$$u\frac{\partial T}{\partial x} + v\frac{\partial T}{\partial y} = \kappa\left(\frac{\partial^2 T}{\partial x^2} + \frac{\partial^2 T}{\partial y^2}\right) \tag{7}$$

and when the velocity components given by equation (6) are inserted, equation (7) written in parabolic co-ordinates reduces to,

$$2\xi\eta'\frac{\partial T}{\partial \xi} - \eta'^2\frac{\partial T}{\partial \eta'} = \frac{\kappa}{A_2 \nu}\left(\frac{\partial^2 T}{\partial \xi^2} + \frac{\partial^2 T}{\partial \eta'^2}\right) \tag{8}$$

where $\eta' = (\eta - Re^{1/2})$. At the crystal tip $\xi = 0$. If we

assume conduction along the streamlines to be much less than conduction across them,

$$\frac{\partial^2 T}{\partial \xi^2} \ll \frac{\partial^2 T}{\partial \eta'^2},$$

equation (8) reduces to,

$$\frac{\kappa}{A_2 v}\frac{\partial^2 T}{\partial \eta'^2} + \eta'^2 \frac{\partial T}{\partial \eta'} = 0$$

which can be integrated with boundary conditions $T = T_i$ at $\eta' = 0$ and $T = T_\infty$ at $\eta' = \infty$ to give,

$$\frac{T - T_i}{T_\infty - T_i} = \frac{3}{\Gamma(\frac{1}{3})}\left(\frac{A_2 Pr}{3}\right)^{1/3} \int_0^{\eta'} e^{-(A_2 \eta'^3/3)}\, d\eta'. \quad (10)$$

The corresponding temperature gradient at the surface is given by

$$\left(\frac{\partial T}{\partial \eta'}\right)_{\eta'=0} = \frac{3}{\Gamma(\frac{1}{3})}\left(\frac{A_2 Pr}{3}\right)^{1/3}(T_\infty - T_i) \quad (11)$$

or in Cartesian co-ordinates, at the tip ($x = -R/2$, $y = 0$; $\xi = 0$, $\eta = Re^{1/2}$)

$$\frac{\partial T}{\partial x} = \frac{1}{R}(Re)^{1/2}\frac{3}{\Gamma(\frac{1}{3})}\left(\frac{A_2 Pr}{3}\right)^{1/3}(T_i - T_\infty). \quad (12)$$

The crystal growth rate is related to the heat transfer into the flow at the tip by the equation

$$v = \frac{k_s}{\rho_i L}\left(\frac{\partial T}{\partial x}\right)$$

$$v = \frac{k_s}{\rho_i L}\frac{Re^{1/2}}{R}\frac{3}{\Gamma(\frac{1}{3})}\left(\frac{A_2 Pr}{3}\right)^{1/3}(T_i - T_\infty)$$

which may be rewritten in the form

$$\frac{v}{V} = \left(\frac{\rho_s}{\rho_i}\right)\left(\frac{\kappa}{v}\right)\frac{3}{\Gamma(\frac{1}{3})}\left(\frac{A_2 Pr}{3}\right)^{1/3}\left(\frac{v}{VR}\right)^{1/2} \times \frac{C_p[\Delta T - (\beta/R)]}{L} \quad (13)$$

where, as in equation (3) allowance is made for the effect of curvature of the crystal tip.

Optimizing the growth rate with respect to R gives

$$\frac{v}{V} = \frac{2}{3}\left(\frac{\rho_s}{\rho_i}\right)\left(\frac{\kappa}{v}\right)\frac{3}{\Gamma(\frac{1}{3})}\left(\frac{A_2 Pr}{3}\right)^{1/3} \times \left(\frac{\rho_i L v \Delta T}{3\gamma T_m V}\right)^{1/2}\frac{C_p \Delta T}{L} \quad (14)$$

giving the form $v \propto V^{1/2}\Delta T^{3/2}$.

When the ice crystals grow in a flowing stream of brine the salt concentration which tends to build up at the crystal tip must diffuse away from the ice surface.

The mass fraction gradient at the crystal is then obtained by replacing the Prandtl number (Pr) in equation (12) by the Schmidt number (Sc) or

$$\frac{\partial W}{\partial x} = \frac{3}{\Gamma(\frac{1}{3})}\frac{Re^{1/2}}{R}\left(\frac{A_2 Sc}{3}\right)^{1/3}(W_i - W_\infty). \quad (15)$$

A salt balance at the crystal tip gives, [5]

$$\rho_s D\frac{\partial W}{\partial x} = v\rho_i W_i \quad (16)$$

where ρ_s is the density of the salt solution, giving

$$v = \frac{3}{\Gamma(\frac{1}{3})}\frac{D}{R}(Re)^{1/2}\left(\frac{A_2 Sc}{3}\right)^{1/3}\left(\frac{\rho_s}{\rho_i}\right)\left(1 - \frac{W_\infty}{W_i}\right). \quad (17)$$

Using the binomial theorem, equation (17) can be solved for the interfacial salt concentration as

$$\frac{W_i}{W_\infty} = 1 + \left(\frac{3}{A_2}\right)^{1/3}\frac{\Gamma(\frac{1}{3})}{3}\frac{(\rho_i/\rho_s)}{Re^{1/2}Sc^{1/3}}\frac{vR}{D}. \quad (18)$$

If the temperature driving force in equation (13) is modified to allow for the effect of salt depressing the melting point so that $[\Delta T - (\beta/R)]$ becomes $[\Delta T - \lambda W_i - (\beta/R)]$ and if W_i is eliminated from the resultant equation and equation (18) then the rate of growth of the ice crystal is given by,

$$\frac{v}{V} = \left(\frac{\rho_s}{\rho_i}\right)\left(\frac{\kappa}{v}\right)\frac{3}{\Gamma(\frac{1}{3})}\frac{(A_2 Pr/3)^{1/3}}{1 + 0{\cdot}93\left(\frac{\kappa}{D}\right)^{2/3}\frac{C_p \lambda W_\infty}{L}} \times \left(\frac{v}{VR}\right)^{1/2}\frac{C_p[\Delta T_s - (\beta/R)]}{L}. \quad (19)$$

When the equation is optimized for maximum growth rate with respect to R it becomes

$$\frac{v}{V} = 2\left(\frac{\rho_s}{\rho_i}\right)\left(\frac{\kappa}{v}\right)\left(\frac{A_2 Pr}{3}\right)^{1/3}\frac{1}{1 + 0{\cdot}93\left(\frac{\kappa}{D}\right)^{2/3}\left(\frac{C_p \lambda W_\infty}{L}\right)} \times \left(\frac{\rho_i L v \Delta T_s}{3\gamma T_m V}\right)^{1/2}\left(\frac{C_p \Delta T_s}{L}\right). \quad (20)$$

Thus equation (20) is the final equation for the A-axis growth of an ice crystal with the transfer of heat and diffusion of salt away from the tip into the creeping brine.

This theory depends on the numerically determined coefficient A_2 in the velocity distribution expression given by equation (6). To the extent that this constant has no simple analytical source the theory is unsatisfactory. Consequently, a second theory which also avoids the unsatisfactory aspects of the forward stagnation point laminar boundary-layer theory was developed and is outlined below.

4.3 *Ice conduction model*

In this theory it is assumed that the heat generated at the growth front is conducted along the crystal and then removed by forced convection, at right angles to the growth direction from the large flat faces of the crystal. This model is made physically plausible by the fact that the thermal conductivity of ice is four times that of water.

Consider first the growth of the ice crystal in a flowing stream of pure water. The crystal is assumed to be in the form of a parabolic cylinder, as shown in Fig. 5, of thickness $2t$ at distance x from the origin which is now taken at the front stagnation point, rather than at the focus as before. Because the C-axis growth rate of ice crystals is much less than the A-axis growth rate, it is assumed that the crystal is thin with the radius of curvature R of the front stagnation point so small

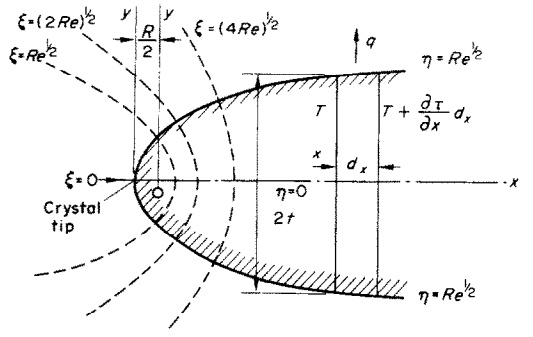

FIG. 5. Parabolic tip of ice crystal.

that the temperature can be taken as uniform across each section of the crystal, i.e.

$$\frac{\partial T}{\partial y} \ll \frac{\partial T}{\partial x}.$$

The equation of the crystal surface is of the form,

$$t^2 = 4ax \tag{21}$$

where the constant $a = \frac{1}{2}R$. Thus,

$$t = \sqrt{(2Rx)}. \tag{22}$$

Now the heat convected from the surface of a flat plate with temperature $T_i(x)$ varying with distance x from the leading edge is given by [15]

$$q = -0{\cdot}66\frac{k_l}{x}(Pr)^{1/3}(Re_x)^{1/2} \times\left[\int_0^x \frac{\theta_i'(\phi)\,\mathrm{d}\phi}{[1-(\phi/x)^{3/4}]^{1/3}} + (T_i - T_\infty)_{x=0}\right]. \tag{23}$$

By writing a heat balance on the element of the thin parabola shown in Fig. 5,

$$k_i\frac{\partial}{\partial x}\left|2t\frac{\partial T_i(x)}{\partial x}\right|\mathrm{d}x = q\,\mathrm{d}x. \tag{24}$$

Combining equations (16) and (17)

$$A_3\left(\frac{\mathrm{d}\theta_i}{\mathrm{d}x} + 2x\frac{\mathrm{d}^2\theta_i}{\mathrm{d}x^2}\right) = \int_0^x \frac{\theta_i'(\phi)\,\mathrm{d}\phi}{\{[1-(\phi/x)^{3/4}]\}^{1/3}} + \theta_{i0} \tag{25}$$

where

$$\theta_i = (T_i - T_\infty),$$

and

$$A_3 = \left(\frac{\sqrt{2}}{0{\cdot}66}\right)\left(\frac{k_i}{k_l}\right)\frac{R}{(Pr)^{1/3}(Re)^{1/2}}. \tag{26}$$

The integral equation (18) was solved by assuming,

$$\theta_i = \theta_{i0} + a_i x + a_2 x^2 + a_3 x^3 + \ldots$$

in which case,

$$A_3(a_1 + 6a_2 x + 15a_3 x^2 + \ldots) = -[\theta_{i0} + \tfrac{4}{3}a_1\beta(\tfrac{4}{3},\tfrac{2}{3})x + \tfrac{8}{3}a_2\beta(\tfrac{8}{3},\tfrac{2}{3})x^2].$$

By equating coefficients,

$$\frac{\theta_i}{\theta_{i0}} = 1 - \alpha_1\frac{x}{A_3} + \alpha_2\left(\frac{x}{A_3}\right)^2 - \alpha_3\left(\frac{x}{A_3}\right)^3 \tag{27}$$

where

$$\alpha_1 = 1;\quad \alpha_2 = (\tfrac{2}{9})\beta(\tfrac{4}{3},\tfrac{2}{3});\quad \alpha_3 = (\tfrac{8}{45})(\tfrac{2}{9})\beta(\tfrac{4}{3},\tfrac{2}{3})\beta(\tfrac{8}{3},\tfrac{2}{3}) \tag{28}$$

and $\beta(p,q)$ is the Beta function. The crystal growth rate v is related to the heat transferred away from the tip by the equation

$$v = \frac{k_i}{\rho_i L}\left(\frac{\partial T_i}{\partial x}\right)_{x=0} = \frac{k_i}{\rho_i L}\left(\frac{\partial \theta_i}{\partial x}\right)_{x=0}.$$

Using equation (21),

$$v = -\left(\frac{k_i}{\rho_i L}\right)\frac{\theta_{i0}}{A_3}$$

i.e.

$$\frac{v}{V} = \frac{0{\cdot}66}{\sqrt{2}}\left(\frac{\rho_s}{\rho_i}\right)\frac{\kappa}{\nu}(Pr)^{1/3}\left(\frac{\nu}{VR}\right)^{1/2}\frac{C_p[\Delta T - (\beta/R)]}{L} \tag{29}$$

where

$$\theta_{i0} = (T_{i0} - T_\infty) = (T_m - T_\infty) - (\beta/R) = \Delta T - (\beta/R). \tag{30}$$

If this is optimized with respect to R,

$$\frac{v}{V} = \frac{0{\cdot}66}{\sqrt{2}}\left(\frac{2}{3}\right)\left(\frac{\rho_s}{\rho_i}\right)\frac{\kappa}{\nu}(Pr)^{1/3}\left(\frac{\rho_i L v\Delta T}{3\gamma T_m V}\right)^{1/2}\left(\frac{C_p\Delta T}{L}\right) \tag{31}$$

giving once again $v \propto V^{1/2}\Delta T^{3/2}$.

For the ice/water system $A_3 \approx 100R$ and this value together with the rapid decrease in the values of the coefficients suggest that an estimation of the distance x_1 over which conduction in the ice crystal takes place can be obtained using only the first two terms of the series expansion of equation (27) with $\theta_i = 0$ giving

$$x_1 = A_3/\alpha_1$$

and

$$\frac{x_1}{R} = \frac{\sqrt{2}}{0{\cdot}66}\frac{k_i}{k_l}Pr^{-1/3}Re^{-1/2}. \tag{32}$$

For the ice/water system, this implies $x_1/R \approx 100$ and with $R = 20\times10^{-6}$ cm, $x_1 \approx 20\times10^{-4}$ cm.

Allowing for diffusion of the salt into the creeping flow around the tip in the same manner as for the previous model the rate of growth of the ice crystal is given by

$$\frac{v}{V} = \frac{0{\cdot}66}{\sqrt{2}}\left(\frac{\rho_s}{\rho_i}\right)\left(\frac{\kappa}{\nu}\right)\frac{Pr^{1/3}}{1+0{\cdot}93\left(\frac{\kappa}{D}\right)^{2/3}\frac{C_p\lambda W_\infty}{L}} \times\left(\frac{\nu}{VR}\right)^{1/2}\frac{C_p[\Delta T_s - (\beta/R)]}{L} \tag{33}$$

which when optimized for maximum growth rate gives,

$$\frac{v}{V} = \frac{2}{3}\left(\frac{0{\cdot}66}{\sqrt{2}}\right)\left(\frac{\rho_s}{\rho_i}\right)\left(\frac{\kappa}{\nu}\right)\frac{Pr^{1/3}}{1+0{\cdot}93\left(\frac{\kappa}{D}\right)^{2/3}\frac{C_p\lambda W_\infty}{L}} \times\left(\frac{\rho_i L v\Delta T_s}{3\gamma T_m V}\right)^{1/2}\frac{C_p\Delta T_s}{L} \tag{34}$$

which is similar in form to equations (5) and (20) and is the final expression for the A-axis growth of an ice crystal with heat transfer along the crystal away from the tip and then through the boundary layer on the

flat faces into the main brine stream and with diffusion of the salt away from the tip into the creeping brine.

The ice conduction model implies that the ice crystal temperature decreases from the tip and means that the ice surface temperature away from the tip is not at the local equilibrium temperature. While this conflicts with most existing theories it is thought to be reasonable that, although the tip may be at the local equilibrium freezing temperature other parts of the crystal might be sub-cooled.

In practice, it is possible that both the creeping flow and ice conduction models would operate simultaneously. In this event, the temperature distribution through the crystal and around the tip should alter, thereby reducing the effect of each mechanism and probably giving a growth rate comparable to that obtained by either mechanism operating alone.

5. COMPARISON OF THEORY AND EXPERIMENT

For pure water, both the creeping flow theory summarized by equation (14) and the ice conduction theory summarized by equation (31) imply a growth law which satisfies equation (2) the constant of proportionality for creeping flow theory is 0·74 times and for the ice conduction theory 0·68 times the value given by the simple stagnation flow boundary-layer theory of equation (3).

As shown in Fig. 2(c) the experimental results agree much better with either model than with the boundary-layer model even when a reasonable value of $\gamma = 22$ mJ/m^2 is used whilst removing the anomaly of using boundary-layer theory at very low front stagnation point Reynolds numbers. Consequently, for pure water either model seems to provide a more satisfactory theory of A-axis growth than the boundary-layer model.

When diffusion of the salt from the ice tip in creeping flow is added to the models resulting in equations (20) and (34), the agreement between theory and experiment is less good. Comparison between Barduhn's theory equation (3), the new theories equations (20) and (34) and the experimental growth rates for a fixed sub-cooling of 1·0 K and a fixed stream velocity of 5 cm/s is made in Fig. 6. None of the theories predict the maximum in the ice growth rate when γ is taken to be constant at 22 mJ/m^2 and, with increase in salt concentration all theories show a continuous fall in growth rate, although beyond the maximum the rate of this fall is lower than that observed experimentally. The later models show some improvement over their predecessor, largely because of better agreement with pure water. However, when γ varies with concentration according to the measurement of Wood [16], implying a slight minimum in γ at 0·5 per cent concentration, a maximum in the growth rate/concentration curve at about the measured concentration of 0·5 per cent is observed. As Fig. 6 shows, this theoretical maximum is much less than the measured maximum in the ice growth rate curve. However, even this partial explanation of the growth rate maximum, coincident as it is with the interfacial tension minimum at the same

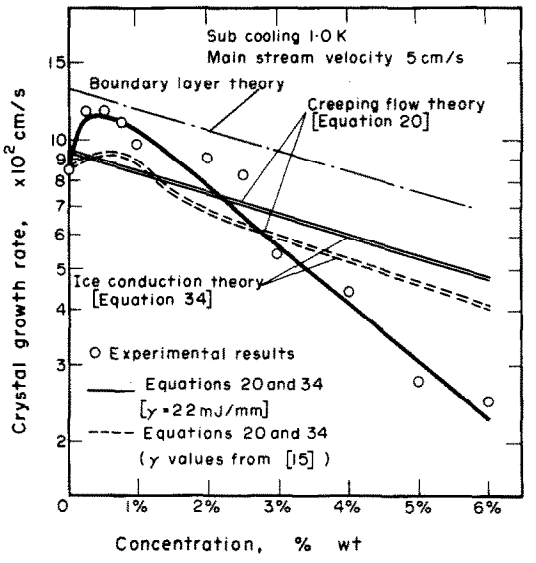

FIG. 6. Comparison of experimental growth rates, ice conduction theory and laminar boundary-layer theory.

concentration, must be viewed with suspicion because no satisfactory physical interpretation has been given of Wood's data.

6. CONCLUSIONS

1. The experimental results for A-axis growth rate for pure water and for brine solutions with sub-cooling greater than about 0·4 K are in reasonable agreement with previously published data.

2. The theoretical work outlined here suggests that this growth rate of ice in pure water is controlled by heat transfer, either from the crystal tip with creeping flow or by heat transfer from the flat surfaces of the ice crystal. The new theories predict $v \propto V^{1/2}\Delta T^{3/2}$, as found experimentally, but remove the anomalies of front stagnation point boundary layer and enable a more realistic value of $\gamma = 22$ mJ/m^2 to be used.

3. The new heat-transfer theories, when combined with a salt diffusion allowance for brine concentration, also gives an improved estimate of growth rates in saline solutions, but the experimental effect of salt concentration is not explained in detail unless a stronger minimum is possible in the γ/concentration curve than hitherto found.

Acknowledgement—This work forms part of a research contract on Background Research in Desalination Technology supported by the Science Research Council of Britain.

REFERENCES

1. J. Deans, The A-axis growth of ice crystals in flowing saline solutions, Ph.D. thesis, University of Strathclyde, Glasgow (1972).
2. L. A. Bukina, The rate of growth of frazil ice crystals, *Bull. Acad. Sci. USSR, Geophys. Ser. No.* 12, 1165–1168 (1962).
3. J. Farrar and W. S. Hamilton, Nucleation and growth of ice crystals, O.S.W. Res. and Dev. Report No. 127 (1965).
4. R. Fernandez, The growth of ice in flowing water and NaCl solutions, Ph.D. thesis, Syracuse University, New York (1967).

5. R. Fernandez, The growth of ice in flowing subcooled solutions, O.S.W. Res. and Dev. Report No. 333 (1968).
6. H. C. Simpson *et al.*, The growth of ice crystals, in *Proc. of 4th International Symposium on Fresh Water from the Sea*, Vol. 3, pp. 395–407. Heidelberg (1973).
7. J. Poisot, The growth rate of ice crystals in flowing subcooled water, O.S.W. Res. and Dev. Report No. 370 (1968).
8. J. G. Vlahakis, The anomalous growth rate of ice crystals in flowing water and NaCl solutions, O.S.W. Res. and Dev. Report No. 830 (1972).
9. V. G. Tamman and A. Z. Buchner, *Anorg. Allg. Chem.* **222**, 371–381 (1935).
10. R. B. Bird, W. E. Stewart and E. N. Lightfoot, *Transport Phenomena*. Wiley, New York (1966).
11. C. S. Lindenmeyer, The solidification of super-cooled aqueous solutions, Ph.D. thesis, Harvard University (1969).
12. G. K. Batchelor, *An Introduction to Fluid Dynamics*. Cambridge University Press, Cambridge (1967).
13. R. T. Davies, Numerical solution of the Navier–Stokes equation for symmetric laminar incompressible flow past a parabola, *J. Fluid Mech.* **51**, 417 (1972).
14. S. R. C. Dennis and J. D. Walsh, Numerical solutions for steady symmetric viscous flow past a parabolic cylinder in a uniform stream, *J. Fluid Mech.* **50**, 801 (1971).
15. G. R. Wood, Kinetics of ice crystal nucleation from water and electrolyte solutions, O.S.W. Res. and Dev. Report No. 500 (1971).
16. J. Nakamura, Experimental investigation of the *A*- and *C*-axis growth of ice crystals, M.Sc. thesis, University of Strathclyde, Glasgow (1972).